https://doi.org/10.35336/VA-1493 https://elibrary.ru/OKSIXQ

ATRIAL FIBRILLATION DETECTION USING MACHINE LEARNING ALGORITHM FROM SINGLE LEAD ELECTROCARDIOGRAMS

N.Trong Tuyen[1], H.Thi Yen[1], N.Manh Cuong[1], D.Tran Huy[1], L.Hong Hai[2], T.Thi Nhan[3], V.Tri Tiep[1]

[1]Le Quy Don Technical University, Vietnam, Hanoi, 236 Hoang Quoc Viet; [2]Vietnam Ministry of Health, Vietnam, Hanoi, 135/1 Nui Truc; [3]Electric Power University, Vietnam, Hanoi, 235 Hoang Quoc Viet

Aim. Atrial fibrillation (AF) represents one of the most critical cardiac arrhythmias, as it significantly increases the risk of stroke. Its detection is particularly challenging due to the unpredictable nature of its episodes.

Methods. This study proposes a low-complexity algorithm, enabling integration into embedded devices for real-time AF episode detection. The proposed method integrates non-linear, time-domain and frequency-domain features extracted from electrocardiogram signals with The LightGBM algorithm (an extension of decision tree algorithm) is used to classify and detect AF.

Results. The model was trained using the MIT-BIH AF Database (MIT-AFDB), achieving sensitivity (*Se*), specificity (*Sp*), accuracy rates (*Acc*), precision (*PPV*), F1-score and AUC of 0.9838, 0.9690, 0.9748, 0.9543, 0.9688 and 0.9957, respectively. We also performed 10-fold cross-validation on this dataset. The obtained values for *Se*, *Sp*, *Acc*, *PPV*, F1-score, and AUC were, respectively, 0.9837 ± 0.0020, 0.9701 ± 0.0021, 0.9755 ± 0.0007, 0.9559 ± 0.0029, 0.9696 ± 0.0008, and 0.9959 ± 0.0002. This indicates that the model achieves good performance compared to current studies in AF recognition and detection.

Conclusions. The experimental results demonstrate that the model achieves high performance in the classification and detection of AF episodes. Furthermore, the model is suitable for integration into real-time arrhythmia detection systems.

Key words: electrocardiogram; atrial fibrillation; heart rate variability; QT interval variability; power spectrum; machine learning

Conflict of interest: none.
Funding: none.
Aknowledgement: The article is an output of the regular research (2024) at Le Quy Don Technical University, code number 24.1.69'.
Received: 26.03.2025 **Revision received:** 12.05.2025 **Accepted:** 13.05.2025
Corresponding author: Nguyen Trong Tuyen, Email: nguyentuyen1988@gmail.com

N.Trong Tuyen - ORCID ID 0000-0001-9408-2622, H.Thi Yen - ORCID ID 0000-0003-4431-0804, N.Manh Cuong - ORCID ID 0000-0002-7665-6503, D.Tran Huy - ORCID ID 0009-0004-7037-051, L.Hong Hai - ORCID ID 0009-0002-2363-0120, T.Thi Nhan - ORCID ID 0009-0002-3760-6607, V.Tri Tiep - ORCID ID 0000-0002-5868-018X

For citation: Tuyen Trong N, Thi Yen H, Manh Cuong N, Tran Huy D, Hong Hai L, Thi Nhan T, Tri Tiep V. Atrial fibrillation detection using machine learning algorithm from single lead electrocardiograms. *Journal of Arrhythmology.* 2025;32(2): 27-32.

Atrial fibrillation (AF), a life-threatening cardiac arrhythmia, has shown a significant global burden, with its prevalence rising from 33.5 million cases in 2010 to 59 million in 2019. Projections estimate a twofold to threefold increase by 2050, particularly among high-risk populations such as hypertensive and diabetic patients. AF is characterized by uncoordinated atrial electrical activity, leading to thrombus formation and elevated stroke risk [1]. Clinically, AF is categorized into paroxysmal, persistent, and permanent subtypes, with the latter posing significant management challenges due to irreversible rhythm disturbances.

Current diagnostic methods, including Holter monitoring, exhibit limitations in detecting transient AF episodes, underscoring the need for advanced monitoring systems. Recent advancements in wearable devices and artificial intelligence have enhanced real-time AF detection; however, demonstrating their effectiveness in detecting short AF episodes lasting less than 30 seconds remains a challenging problem. These AF episodes have the potential to develop into longer, more persistent episodes, which are more difficult to restore to normal sinus rhythm (NSR). Electrocardiogram (ECG)-based machine learning models leverage AF-associated markers, such as RR interval irregularity and fibrillatory wave morphology, to improve classification accuracy. Prior studies have employed Markov chains, spectral analysis, and entropy metrics on RR intervals [2-4], while others have integrated atrial activity frequency features [5, 6]. Deep learning approaches, in which convolutional neural networks (CNNs) are used to automatically extract features with filters that have been investigated in recent years, have also been explored. In study [7], the authors used segments comprising 30 RR intervals from the MIT-AFDB, combining CNN and Long-Short Term Memory (LSTM) networks to extract high-level features for the classification of AF and NSR. The model achieved sensitivity and specificity of 98.98% and 96.95%, respectively. In study [8], the authors used segments with a duration of 750 ms - comprising 250 ms before the R peak and 500 ms after the R peak - as input data for a machine learning model employing a hybrid CNN-LSTM network to classify AF and other cases, achieving sensitivity and specificity of 97.87% and 99.29%, respectively. Additionally, some models transform biosignal data

into 2D images, which are then fed into CNNs to recognize AF and NSR, as demonstrated in studies [9, 10]. However, these models require large amounts of input data and powerful computational resources that, in some cases, exceed those available on conventional computing devices.

The development of algorithms that utilize the selection of pathological features from ECG signals based on time-domain and frequency-domain characteristics is of considerable significance. These models facilitate a reduction in the number of input features and require less training data compared to deep learning models, making them more suitable for real-time applications. In this study, we propose a method that incorporates time-domain features, nonlinear features of heart rate variability (HRV), and the morphological characteristics of atrial activity in cases of AF and NSR, along with frequency-domain features for the identification and detection of AF episodes. The model was developed using the MIT-AFDB and validated on the SHDB-AF Database (SHDB-AF). Furthermore, the implementation of the LightGBM algorithm enhances the model's applicability in real-time systems for AF recognition and detection.

METHODS

Outline of proposed method

In this study, we propose a methodology that incorporates HRV, time- and frequency-domain features alongside a machine learning model to classify and detect AF using ECG signals. The feature set construction process in the proposed algorithm consists of the following steps: signal preprocessing, which includes signal selection, filtering, and analysis; computation of HRV features in the time domain; calculation of frequency-domain features; construction of the machine learning model; and evaluation of its performance.

The classification and detection algorithm are designed for single-channel ECG signals. To compute time-domain and frequency-domain features, the ECG signal first undergoes noise filtering. Subsequently, feature extraction is performed by isolating characteristic waves of the ECG signal, including the QRS complex, P wave, and T wave. HRV features, encompassing time-domain and nonlinear characteristics, are identified. Additionally, atrial waveform morphology features in cases of AF and NSR are determined through QT intervals on the ECG signal. Frequency-domain features are extracted by analyzing the peak energy spectral distribution under varying conditions. Finally, the LightGBM algorithm is utilized to classify ECG signals into two categories: AF and non-AF.

Signal preprocessing

Elimination of baseline drift noise was achieved using a median filter [11]. Following the removal of baseline drift, a Savitzky-Golay smoothing filter was applied for mitigating high-frequency noise [12]. Both the median filter and the Savitzky-Golay filter preserve the morphology of the ECG signal, ensuring that the original signal characteristics remain unchanged. After denoising the ECG signal, premature ventricular complexes and premature atrial complexes were removed based on the length of the RR interval. Detection is based on the criterion that the distance from the R peak of abnormality to the preceding R peak is less than 0.8 times the average RR interval.

ECG signals were subsequently segmented, including QRS complexes and T-wave endpoints. Detection of QRS complexes was performed using the Pan-Tompkins algorithm [13]. This algorithm identifies QRS complexes through filtering and thresholding techniques for locating R-peaks. Positions of the Q and S waves were determined relative to the R-wave positions. Identification of T-wave positions was carried out using the Zhang algorithm, which leverages the convexity or concavity of the T-wave [14].

The primary advantage of these waveform segmentation algorithms lies in their low computational complexity and high effectiveness in detecting ECG waveforms. Thus, they are well-suited for real-time analysis and recognition of ECG signals.

Heart rate variability features

AF is characterized by irregular RR intervals. Consequently, HRV features play a crucial role in detecting AF. In this study, statistical features of RR intervals, including the mean, range, and dispersion, were utilized as inputs for the machine learning model. These parameters are defined by Eq. (1), (2), and (3), as follows.

$$RR_{mean} = \frac{\sum_{i=1}^{N_b} RR_i}{N_b} \quad (1)$$

$$dRR = RR_{max} - RR_{min} \quad (2)$$

$$dispRR = \sqrt{\frac{\sum_{i=1}^{N_b}(RR_i - RR_{mean})^2}{N_b - 1}} \quad (3)$$

The non-linear features of HRV analyzed include the SD1 and SD2 parameters derived from the Poincaré plot, and the ellipse area defined by the SD1 and SD2 axes. These parameters provide insights into HRV, with SD1 reflecting short-term variability and SD2 representing long-term variability. The irregularity of RR intervals is evident in the scattergram of RR intervals, distinguishing cases of AF from NSR. The SD1 and SD2 values and area of ellipse are calculated using Eq. (4), (5) and (6), respectively.

$$SD_1 = \sqrt{\frac{Var(RR_{n+1} - RR_n)}{2}} \quad (4)$$

$$SD_2 = \sqrt{\frac{Var(RR_{n+1} + RR_n)}{2}} \quad (5)$$

$$Area_{SD} = \pi SD_1 SD_2 \quad (6)$$

where the *Var* functions correspond to the variance function of the respective variable of the function.

Time-domain features

In the case of patients with AF, small-amplitude atrial *f* waves with varying frequencies and shapes appear on the ECG signal. The QT interval is the wave interval measured from the end of the T wave to the start of the QRS complex (QRS onset). These points are determined using the algorithms mentioned above. Subsequently, the synchronization of the signal intervals is performed using interpolation methods to assess the variability of the QT interval in both AF and NSR cases.

Due to changes in the relative position of the Q wave with respect to the R peak, the position of the P wave peak

in some cases also changes within the analysis window. Therefore, when synchronizing the QT intervals in the case of NSR, we account for the position of the P wave peak. The probability of detecting the P peak is expressed through the following conditions: (i) the P peak appears within 180 ms before the R peak and (ii) the amplitude of the P wave is not less than 0.02 times the average amplitude of the R wave in the signal analysis window. If P peaks satisfying both of two conditions (i) and (ii), the QT intervals within the analysis window are synchronized through interpolation using three points of the largest QT interval: the endpoint of T wave, the QRS onset point, and the peak of the QT interval or the P wave peak. In the opposite case, the QT intervals are synchronized through interpolation using only the endpoint of T wave and the QRS onset points of the largest QT interval. The feature used to determine the presence of the P wave on the QT interval is defined by Eq. (7), (8) and (9), as follows.

$$\overline{TQ} = \frac{\sum_{i=1}^{N_b} TQ_i}{N_b} \quad (7)$$

$$D_e = \frac{\|TQ_i - \overline{TQ}\|}{\|TQ_i\|} \quad (8)$$

$$Var_{De} = \frac{N_{D_e \geq D_{th}}}{N_b} \quad (9)$$

where, *TQi* represents the QT intervals in the monitored signal segment after synchronization, $\overline{TQ}$ is the average value of the *TQi* intervals, $N_{De \geq Dth}$ is the number of D_e values greater than a specified threshold D_{th} (in this study, D_{th} is empirically determined to be 0.8), N_b is the number of QT intervals after excluding premature ventricular beats and premature atrial beats, and || || denotes the length of a vector.

Frequency-domain features

In this study, the power spectral distribution is utilized as a feature for identifying and classifying AF and NSR. The power spectrum is computed using a method that eliminates spectral leakage at the main spectral peaks of the signal's power spectrum. This approach enables the identification of peak distribution based on clear separation in the signal's power spectrum. The process involves multiplying the signal with appropriate windows. It can be observed that, in the case of NSR, the power spectral peaks are evenly distributed due to the stability of the ECG signal. Assume a sequence of spectral peaks $\{f_i^{PS}\}$ is obtained, where *i = 1,2,...M +1*, and *M + 1* represents the number of spectral peaks within the frequency range [0,15 Hz]. The frequency-domain feature is defined as the variance of the sequence $\delta_i^{PS} = f_{i+1}^{PS} - f_i^{PS}$, for $1 \leq i \leq M$, as determined by Eq. (10).

$$\sigma_p^{PS} = Var(\delta_i^{PS}) = \sqrt{\frac{1}{M-1}\sum_{i=1}^{M}(\delta_i^{PS} - \overline{\delta^{PS}})^2} \quad (10)$$

where, $\overline{\delta^{PS}}$ represents the mean value of the sequence δ_i^{PS}.

The distribution of peaks is determined based on the power spectrum of the signal, independent of the detection of the ECG's R peak. Therefore, this approach is particularly beneficial in scenarios where the signal remains stable during NSR but is affected by noise, especially when the R peak has a lower amplitude compared to other waveform peaks. In such instances, we determine the variability values of the non-linear HRV features similarly to those defined in Eq. (4), (5), and (6). Variations in the peak spectral distribution are calculated according to Eq. (11), (12), and (13) as follows.

$$\sigma_{SD1} = \sqrt{\frac{Var(\delta_{n+1}^{PS} - \delta_n^{PS})}{2}} \quad (11)$$

$$\sigma_{SD2} = \sqrt{\frac{Var(\delta_{n+1}^{PS} + \delta_n^{PS})}{2}} \quad (12)$$

$$Area_\sigma = \pi \sigma_{SD1} \sigma_{SD2} \quad (13)$$

Table 1.

Classification Features

Feature	Description
RRmean	Mean of RR intervals
dRR	Range of RR intervals
dispRR	Dispersion of RR intervals
SD_1	Short-term variability of HRV
SD_2	Long-term variability of HRV
$Area_{SD}$	Area of the ellipse defined by SD1 and SD2
Var_{De}	Variability of TQ intervals
σ_p^{PS}	Dispersion of ECG signal power spectrum peaks
σ_{SD1}	Modified SD1 of ECG signal power spectral peaks
σ_{SD2}	Modified SD2 of power spectral peaks
$Area_\sigma$	Modified of area of the ellipse defined by SD1 and SD2 of power spectral peaks

Building machine learning model for classification ECG database

The MIT-AFDB comprises 25 records, each containing two ECG signals recorded over durations ranging from 6 to 10 hours at Beth Israel Hospital in Boston. The signals were sampled at a frequency of 250 Hz with an analog-to-digital converter (ADC) resolution of 12 bits. The dataset provides annotations for episodes of AF, NSR, and non-AF arrythmias, including atrial flutter (AFL). Notably, most AF cases in this dataset are classified as paroxysmal AF (PAF) [2, 15]. Apart from recordings 00735m and 03665m, which are unavailable, the remaining recordings were utilized for training and evaluating the machine learning model. The SHDB-AF (Saitama Heart Database Atrial Fibrillation) is an open-source ECG recording database from Japan, consist- ing of 100 patients with PAF [15, 16]. The recordings were collected over approximately 24 hours between November 2019 and January 2022. Data acquisition was performed us- ing a Holter monitor with a sampling frequency of 125 Hz, recording two leads per session according to the CC5 and NASA configurations. The recordings in the database un- derwent preprocessing to remove baseline wander and high- frequency noise and were subsequently unsampled to 200 Hz. The dataset includes five classified rhythm types: AFIB (atrial fibrillation), AFL (atrial flutter), AT (atrial tachycardia),

PAT (other supraventricular tachycardias), NOD (intranodal tachycardias), and N (other rhythms, including NSR).

Classification

We used the MIT-AFDB dataset to train the model. Signal segments were extracted from record 1 for each patient, after which these segments were translationally shifted by q = 300 steps, corresponding to approximately one cardiac cycle at a sampling frequency of 250 Hz. The signals were filtered to remove noise, and features were computed as described in the preceding sections and shown in the Table 1. A total of 685,771 samples were obtained using this method, including 272,032 AF samples and 413,739 non-AF samples.

In this study, the LightGBM algorithm was employed to construct the model. LightGBM is a gradient boosting framework based on decision tree algorithms, designed to enhance model performance and reduce memory usage while effectively handling large-scale data. It incorporates several novel techniques, including Gradient-based One-Side Sampling, which selectively retains cases with steep gradients during training to optimize both memory usage and training time. The advantages of this algorithm include rapid training speed, high training efficiency, robust performance with imbalanced data, ease of parameter tuning, and a reduced risk of overfitting [17].

RESULTS

The MIT-AFDB dataset was partitioned into training and testing sets in a 70%:30% ratio. The computing system utilized comprised an Intel Core i7 12700K CPU (5.2 GHz), a 12 GB GPU (Nvidia GeForce RTX 3060), and 32 GB of RAM. The confusion matrix and ROC curve based on the MIT-AFDB are presented in Fig. 1. The sensitivity (*Se*), specificity (*Sp*), accuracy (*Acc*), precision (*PPV*), F1 score, and AUC are 0.9838, 0.9690, 0.9748, 0.9543, 0.9688, and 0.9957, respectively. We also conducted 10-fold cross-validation. The average values of *Se*, *Sp*, *Acc*, *PPV*, F1 score, and AUC are 0.9837 ± 0.0020, 0.9701 ± 0.0021, 0.9755 ± 0.0007, 0.9559 ± 0.0029, 0.9696 ± 0.0008, and 0.9959 ± 0.0002, respectively. A comparative table and distribution of model metrics across the cross-validation folds are illustrated in Fig. 2.

The model was additionally validated on the SHDB-AF. Segments with a length of 15 seconds were extracted using a sliding window with a step size of 240 samples, corresponding to 1.2 seconds at a sampling frequency of 200 Hz. The total number of samples is 6,740,673, of which 1,201,561 are labeled as AF and the remaining 5,539,112 as non-AF, which were used for model testing. The confusion matrix and ROC curve for the SHDB-AF are presented in Fig. 3. The model performance metrics, including *Se*, *Sp*, *Acc*, *PPV* (Positive Predictive Value) and *FPR* (False Positive Rate), in Table 2 and the ROC curve (AUC = 0.9503) on the SHDB-AF indicate that the proposed model can effectively operate on unseen data.

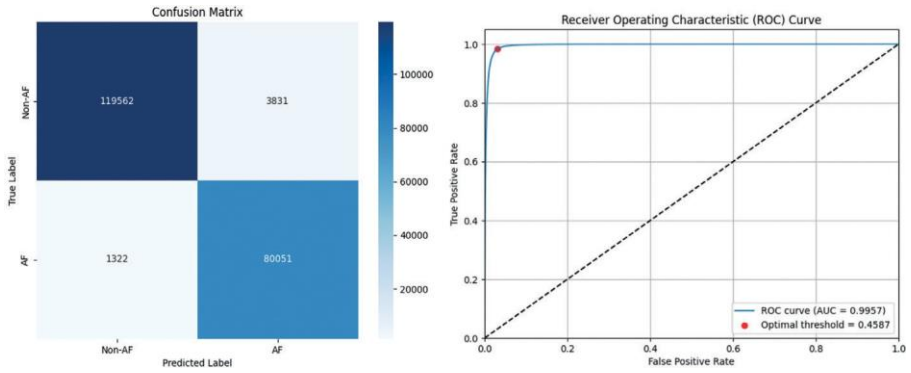

Fig. 1. Confusion matrix for AF classification and AUC curve with MIT-AFDB.

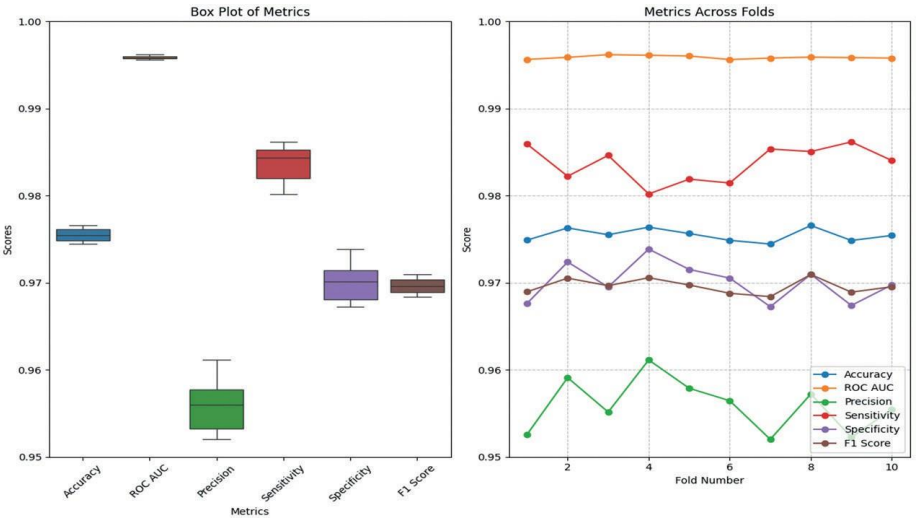

Fig. 2. Model performance metrics across folds in a 10-fold cross-validation of the MIT-AFDB.

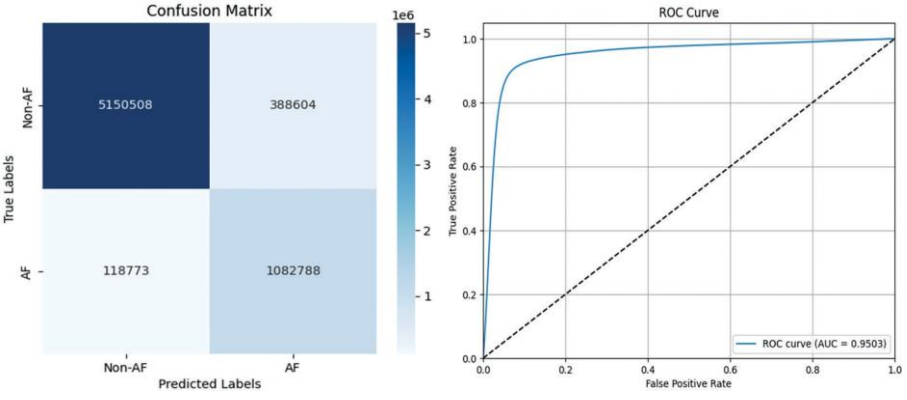

Fig. 3. Confusion matrix and ROC curve for the SHDB-AF.

DISCUSSION

Due to the irregular heart rate in cases of AF, various HRV features are used. Additionally, to assess the presence of atrial waves instead of the typical P-waves, study [20] combines heart rate variability indices (standard deviation of RR intervals, range of RR intervals) with the number of threshold crossings in the atrial wave segment within the QT intervals. Threshold-based parameters are then employed to classify AF and non-AF. In another approach, study [21] proposes using single-parameter wavelet entropy to detect atrial fibrillation by determining the optimal threshold for the wavelet entropy of QT intervals, thereby classifying AF and non-AF. However, this method is sensitive to noise, and variations in QT intervals across ECG signal segments may fluctuate between cardiac cycles, reducing classification accuracy.

Studies that rely on RR interval parameters depend on accurate detection of R-peaks. In many cases, misidentification of R-peaks leads to errors in AF detection. This issue is particularly evident when R-peaks have much lower amplitudes than T-waves. Notable examples include ECG recordings from the MIT-AFDB, specifically in records *04015m*, *04043m*, *04908m*, *04936m*, *06426m*, *06453m*, and *07162m*. In this study, we address these challenges by combining parameters, including RR interval variability, QT interval variability, and the spectral peak distribution in the power spectrum. Calculating QT interval variability based on Eq. (8) helps mitigate the impact of noise on QT interval assessments. Furthermore, computing the spectral peak distribution as a parameter independent of ECG waveform detection enhances the classification accuracy, particularly in cases where R-peak detection is unreliable. This combination of parameters improves the overall specificity, sensitivity, and accuracy of the AF detection algorithm, thereby enhancing its general performance in AF identification.

In recent studies, deep learning models used for AF detection have shown good performance. In study [7], the authors used RR intervals combined with CNN and LSTM networks for feature extraction; our model demonstrates improved performance compared to study [7], with both employing the MIT-AFDB as input. In study [8], the authors utilized raw ECG signals from the MIT-AFDB with CNN and LSTM networks, and our proposed model exhibits higher sensitivity and lower specificity. However, the model in the study [8] has not yet been validated on external unseen data. In study [19], the authors employed signal features and RR intervals from five different databases (CPSC2021, MIT-AFDB, LTAF, MITDB, and NSRDB) and achieved generalization on the training database, but did not extend this generalization to other databases. This study demonstrates that the model performs well across different databases, considering factors such as ethnicity, gender, and lifestyle. The training results obtained using the MIT-AFDB with the LightGBM algorithm and the traditional feature engineering methods compared to recent machine learning models demonstrate that the algorithm achieves performance metrics comparable to those models. Tabl. 3 presents the model performance metrics in comparison with recent studies. Comparative results indicate that the model can classify AF and non-AF with high performance metrics relative to previous studies.

Table 2.

Evaluation metrics of the model on the SHDB-AF

Metrics	SHDB-AF
Se	0.9012
Sp	0.9298
Acc	0.9247
PPV	0.7359
FPR	0.0702

Table 3.

Comparison of the model's performance with other recent deep learning algorithms developed for AF detection

Study	Methods	Evaluation Metrics		
		Sp, %	Se, %	Acc, %
[7]	RR intervals and CNN - LSTM	96.29	98.17	97.10
[8]	ECG beats and CNN - LSTM	99.29	97.87	-
[19]	ECG and RR intervals with Res-CNN and BiLSTM	-	-	98.63
This study	TFE and LightGBM	96.90	98.38	97.48

In the algorithm, low-complexity algorithms are used. This allows the algorithm to be applied in embedded systems for real-time AF detection. The embedded system records ECG signals from leads where f-waves may appear when the patient is in an AF episode. The signals are digitized and transmitted to handheld devices, such as phones, through wireless channels like Bluetooth. These signals are stored in buffers with a length equal to the analysis window length. The features are calculated based on algorithms. The machine learning model is stored in the operating system and predicts the output based on the input features through sliding windows. The sliding windows are shifted by approximately one cardiac cycle compared to the previous window. The machine learning model can also be applied and embedded in edge devices in embedded systems, helping to reduce the load on servers.

Based on the method described above, the start and end points of an AF episode can be determined in real-time, allowing for the calculation of its duration. In real-time monitoring of patients with AF, the duration and frequency of HRV associated with AF are critical factors in both diagnosis and the formulation of treatment plans. These factors provide insight into the progression of the disease. Based on charts displaying the duration and frequency of arrhythmia, healthcare providers can make informed recommendations tailored to the patient's condition. In practice, when acquiring ECG signals from patients, for example, when using home monitoring devices such as Holter or real-time monitoring devices, in some cases, the signals are significantly affected by noise, causing signal distortion. This leads to an inability to recognize the signal. Some patients, in addition to AF, may also have other arrhythmias, such as AFL. These two types of signals can be confusing and can be

misclassified. In future studies, we will continue to develop methods for classifying and recognizing AF with background factors like noise and other arrhythmias.

Limitations

The proposed algorithm faces challenges in accurately detecting AF when the signal quality index of the ECG recording is suboptimal. In such cases, essential ECG waveforms, including the QRS complexes, T waves, and P waves, become indistinct, leading to errors in the detection and classification of AF. The model failed to accurately classify an ECG signal exhibiting junctional rhythm, such as, in record *04013m* of MIT-AFDB. Furthermore, in the case of a patient with AFL and variable F-wave morphology, such as transitions from 2:1 to 3:1 conduction block - the algorithm similarly produced a misclassification. This error is evident in record *07910m* of MIT-AFDB.

CONCLUSIONS

The AF detection algorithm enables the classification and identification of AF as well as NSR. The model employs machine learning techniques that leverage features derived from both the HRV, time-domain and frequency-domain and has been validated using verified databases. Its low computational complexity makes it suitable for integration into real-time AF detection and classification systems. The model is well-suited for implementation in automated ECG signal analysis software for Holter monitors or wearable smart devices designed for home use.

REFERENCE

1. Joglar JA, Chung MK, Armbruster AL et al. 2023 ACC/AHA/ACCP/HRS guideline for the diagnosis and management of atrial fibrillation: a report of the American College of Cardiology/American Heart Association Joint Committee on Clinical Practice Guidelines. *Journals of the American College of Cardiology*. 2024;83(1): 109-279. https://doi.org/10.1016/j.jacc.2023.08.017.
2. Moody GB, Mark RG. A new method for detecting atrial fibrillation using RR intervals. *Computer in Cardiology*. 1983;10: 227-230.
3. Cerutti S, Mainardi LT, Porta A et al. Analysis of the dynamics of RR interval series for the detection of atrial fibrillation episodes. *Computer in Cardiology*. 1997: 77-80. https://doi.org/10.1109/CIC.1997.647834.
4. Horie T, Burioka N, Amisaki T et al. Sample entropy in electrocardiogram during atrial fibrillation. *Yonago Acta Medica.* 2018;61(1): 049-057. https://doi.org/10.33160/yam.2018.03.007.
5. Slocum J, Sahakian A, Swiryn S. Diagnosis of atrial fibrillation from surface electrocardiograms based-on computer-detected atrial activity. *Journal of Electrocardiology.* 1992;25(1): 1-8. https://doi.org/10.1016/0022-0736(92)90123-H.
6. Hirsch G, Jensen SH, Poulsen ES et al. Atrial fibrillation detection using heart rate variability and atrial activity: A hybrid approach. *Expert Systems with Applications.* 2021;169: 114452. https://doi.org/10.1016/j.eswa.2020.114452.
7. Andersen RS, Peimankar A, Puthusserypady S. A deep learning approach for real-time detection of atrial fibrillation. *Expert Systems with Applications*. 2019;115: 465-473. https://doi.org/10.1016/j.eswa.2018.08.011.
8. Petmezas G, Haris K, Stefanopoulos L et al. Automated atrial fibrillation detection using a hybrid CNN-LSTM network on imbalanced ECG datasets. *Biomedical Signal Processing and Control.* 2021;63: 102194. https://doi.org/10.1016/j.bspc.2020.102194.
9. Jun TJ, Nguyen HM, Kang D et al. ECG arrhythmia classification using a 2-D convolutional neural network. *ArXiv preprint arXiv*. 2018;arXiv1804.06812. https://doi.org/10.48550/arXiv.1804.06812.
10. Xu X, Wei S, Ma C et al. Atrial fibrillation beat identification using the combination of modified frequency slice wavelet transform and convolutional neural networks. *Journal of Healthcare Engineering.* 2018;1: 2102918. https://doi.org/10.1155/2018/2102918.
11. Nankani D, Baruah RD. Effective removal of baseline wander from ECG signals: A comparative study, in: *Arup Bhattacharjee, Samir Kr. Borgohain, Badal Soni, Gyanendra Verma, Xiao-Zhi Gao (Eds). Machine Learning, Image Processing, Network Security and Data Sciences: Second International Conference, MIND 2020, Silchar, India, July30-31, 2020, Proceedings, Part II 2, Springer Singapore*. 2020: 310-324.
12. Hargittai S. Savitzky-Golay least-squares polynomial filters in ECG signal processing. *Computer in Cardiology*. 2005: 763-766. https://doi.org/10.1109/CIC.2005.1588216.
13. Pan J, Tompkins WJ. A real-time QRS detection algorithm. *IEEE Transactions on Biomedical Engineering.* 1985;3: 230-236. https://doi.org/10.1109/TBME.1985.325532.
14. Zhang Q, Manriquez AI, Médigue C et al. An algorithm for robust and efficient location of T-wave ends in electrocardiograms. *IEEE Transactions on Biomedical Engineering*. 2006;53(12): 2544-2552. https://doi.org/10.1109/TBME.2006.884644.
15. Goldberger A, Amaral L, Glass L et al. PhysioBank, PhysioToolkit, and PhysioNet: Components of a new research resource for complex physiologic signals. *Circulation [Online]*. 2000;101(23): e215-e220.
16. Tsutsui K, Brimer SB, Ben-Moshe N et al. SHDB-AF: a Japanese Holter ECG database of atrial fibrillation. *ArXiv preprint arXiv*. 2024 Jun;arXiv: 2406.16974. https://doi.org/10.48550/arXiv.2406.16974.
17. LightGBM. Welcome to LightGBM's documentation, 2025. Accessed 5 March 2025 https://lightgbm.readthedocs.io/en/stable/
18. Frazier PI. A tutorial on Bayesian optimization. *ArXiv preprint arXiv*. 2018; arXiv: 1807.02811. https://doi.org/10.48550/arXiv.1807.02811.
19. Zou Y, Yu X, Li S et al. A generalizable and robust deep learning method for atrial fibrillation detection from long-term electrocardiogram. *Biomedical Signal Processing and Control.* 2024;90: 105797. https://doi.org/10.1016/j.bspc.2023.105797.
20. Du X, Rao N, Qian M et al. A novel method for real time atrial fibrillation detection in electrocardiograms using multiple parameters. *Ann. Noninv. Electrocardiol.* 2014;19(3): 217-225. https://doi.org/10.1111/anec.12111.
21. Rodenas J, Garcia M, Alcaraz R et al. Wavelet-entropy automatically detects episodes of atrial fibrillation from single lead electrocardiograms. *Entropy*. 2015;17(9): 6179-6199. https://doi.org/10.3390/e17096179.